AD-A129 914 LECTURES ON MATHEMATICAL COMBUSTION LECTURE 8 COUNTERFLOW DIFFUSION FLAME..(U) CORNELL UNIV ITHACA NY DEPT OF THEORETICAL AND APPLIED MECHAN.. 1/1

UNCLASSIFIED J D BUCKMASTER ET AL. JAN 83 TR-153 F/G 21/2 NL

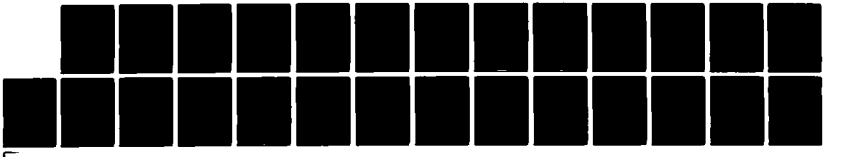

END
DATE FILMED
7-83
DTIC

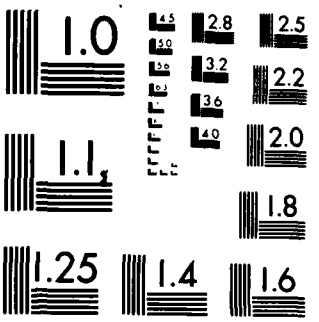

Cornell University

Lecture 8: Counterflow Diffusion Flames

Technical Report No. 153

J.D. Buckmaster & G.S.S. Ludford

January 1983

Theoretical and Applied Mechanics

Thurston Hall

Ithaca, New York

LECTURES ON MATHEMATICAL COMBUSTION

Lecture 8: Counterflow Diffusion Flames

Technical Report No. 153

J.D. Buckmaster & G.S.S. Ludford

January 1983

U.S. Army Research Office
Research Triangle Park, NC 27709

Contract No. DAAG 29-81-K-0127

Cornell University
Ithaca, NY 14853

The view, opinions, and/or findings contained in this report are those of the authors and should not be construed as an official Department of the Army position, policy or decision, unless so designated by other authorized documents.

Contents

		Page
1.	Basic Equations	1
2.	The S-Shaped Burning Response	4
3.	General Extinction Analysis	7
4.	Partial-Burning Branch	11
5.	Stability	12
6.	The Ignition Point	14
	References	16
	Captions	17
	Figures 1-4	18

Lecture 8

COUNTERFLOW DIFFUSION FLAMES

The fundamental characteristic of diffusion flames is that the two reactants, fuel and oxidizer, are supplied in different parts of the combustion field, so that they must come together and mix by diffusion before reaction can take place. Counterflowing streams provide one method of bringing them together; the resulting diffusion flame, whose main properties were established by Liñán, is the subject of this lecture.

1. Basic Equations

Consider the combustion field sketched in figure 1. A stream of gas containing the oxidant $Y_1 = X$ flows to the left and impinges on a stream containing the fuel $Y_2 = Y$ that flows to the right, forming a stagnation point at the origin. The flow field is

$$(u,v) = 2(-x,y) \tag{1}$$

under the constant-density approximation; here a constant of proportionality $\varepsilon/2$, where ε is the straining rate, has been absorbed into the length unit (which is used to define M_r). For such a flow, it is possible for the combustion field to be stratified in the y-direction, with a flat flame sheet at $x = x_*$. The temperature and mass fractions are then functions of x and t alone satisfying, for unit Lewis numbers,

$$L(T) = -2L(X) = -2L(Y) = \Omega \quad \text{with } \Omega = \mathcal{D}XYe^{-\theta/T}; \tag{2}$$

here

$$L \equiv \partial/\partial t - 2x\,\partial/\partial x - \partial^2/\partial x^2 \tag{3}$$

and the boundary conditions are

$$T \to T_{f-},\ X \to 0,\quad Y \to Y_f \text{ as } x \to -\infty,\quad T \to T_{f+},\quad X \to X_f,\ Y \to 0 \text{ as } x \to +\infty. \tag{4}$$

The coefficient $\mathcal{D}$ is proportional to $1/\varepsilon$, so that an increase in the straining rate causes a decrease in $\mathcal{D}$. It is the response of the combustion field to variations in $\mathcal{D}$ that is of principal interest.

Since both Lewis numbers have been taken equal to 1, there are two Shvab-Zeldovich variables (section 2.2), namely

$$T+2X = T_\pm+Z_-,\quad T+2Y = T_\pm+Z_+, \tag{5}$$

where

$$T_\pm = \tfrac{1}{2}[T_{f+}\operatorname{erfc}(-x)+T_{f-}\operatorname{erfc}(x)],\quad Z_- = X_f\operatorname{erfc}(-x),\quad Z_+ = Y_f\operatorname{erfc}(x). \tag{6}$$

Both these variables are annihilated by L and satisfy the boundary conditions (4). We are left with a problem for the temperature alone, when X and Y are hereby suppressed in favor of T. Note that no assumption of steadiness has been made, but these relations can only be applied to unsteady problems for which the initial conditions satisfy the relations. We shall, however, be concerned solely with steady solutions until section 5.

When

$$\mathcal{D}e^{-\theta/T} \to 0 \tag{7}$$

there is no chemical reaction, even if reactants are present, and the combustion is said to be frozen. There are two ways in which this can be brought about:

(i) $\mathcal{D} \to 0$, the small Damköhler-number limit;

(ii) $\mathcal{D} \sim e^{\theta/T_*}$ as $\theta \to \infty$ with $T < T_*$, a creature of activation-energy asymptotics.

In case (i) the entire combustion field is frozen, whereas in case (ii) only that portion where T falls below T_* is frozen.

When

$$\mathcal{D}e^{-\theta/T} \to \infty \tag{8}$$

there is nothing to balance an infinite reaction rate outside vanishingly thin layers (spatial or temporal), and so

$$XY \to 0. \tag{9}$$

At least one of the reactants is not present, i.e. there is equilibrium. Here, as for frozen combustion, there is no reaction, but for quite a different reason.

There are two ways in which equilibrium can be achieved:

(i) $\mathcal{D} \to \infty$, the large Damköhler number limit;

(ii) $\mathcal{D} \sim e^{\theta/T_*}$ as $\theta \to \infty$ with $T > T_*$, another creature of activation-energy asymptotics.

In case (i) the entire combustion field is in equilibrium, but in case (ii) only that portion where T rises above T_* is in equilibrium. Because of the nature of this limit, there is always the possibility of a reaction zone, known as a Burke-Schumann flame sheet, existing in the middle of an equilibrium region; that cannot happen in a frozen region.

Simple analytical treatments are possible in these two limits, frozen and equilibrium. So elementary is the first that we shall forego discussion of it, concentrating instead on the second, which is called the Burke-Schumann (equilibrium) limit after an early, basic combustion problem they considered (see section 10.2). Large values of $\mathcal{D}$ are easily obtained in practice, the reason why the limit was originally introduced by Burke and Schumann.

To the left of the flame sheet at $x = x_*$ there is no oxidant, and to the right no fuel. The Shvab-Zeldovich relations (5) therefore give

$$T = T_{\pm} + \begin{cases} Z_- \\ Z_+ \end{cases}, \quad X = \begin{cases} 0 \\ \frac{1}{2}(Z_- - Z_+) \end{cases}, \quad Y = \begin{cases} \frac{1}{2}(Z_+ - Z_-) \\ 0 \end{cases} \quad \text{for } x \lesseqgtr x_*, \tag{10}$$

and continuity across the flame sheet then requires $Z_- = Z_+$ there, i.e.

$$\operatorname{erf}(x_*) = (Y_f - X_f)/(Y_f + X_f) \tag{11}$$

which determines x_*. The flame sheet lies in the leaner stream: $x_* \lesseqgtr 0$ accordingly as $X_f \gtreqless Y_f$. The flame temperature is

$$T_* = (T_{f-} X_f + T_{f+} Y_f + 2X_f Y_f)/(X_f + Y_f); \tag{12}$$

its structure (35), (36) will be derived in section 3 (for $\theta \to \infty$).

2. The S-Shaped Burning Response

The usual way of characterizing the solution is to plot variations in some significant parameter, such as the maximum temperature, with the Damköhler number. If $T_{f\pm}$, X_f, Y_f are such that the combustion generates a heat flux to both far fields, this response is S-shaped in the limit $\theta \to \infty$(figure 2). Certain physical conclusions can then be drawn.

If the system is in a state corresponding to a point on the lower branch, and $\mathcal{D}$ is slowly increased, the solution can be expected to change smoothly until the point I is reached. Rapid transition to the upper branch will then presumably occur, corresponding to ignition. A subsequent slow decrease in $\mathcal{D}$ is likewise anticipated to produce a smooth decrease in burning rate until extinction occurs at E.

If one of the far fields loses heat, the response is monotonic, so that the phenomena of ignition and extinction are absent. For high activation energy the transition from a monotonic to an S-shaped response occurs when the temperature gradient on one side of the flame sheet is small, a case that is not difficult to analyze.

Assume, without loss of generality, that

$$T_{f+} > T_{f-}; \tag{13}$$

then the small temperature gradient must be on the right of the flame sheet, i.e. hotter side. If it were on the colder side, the flame temperature (12) would be close to T_{f-}, which implies (in the limit of zero gradient)

$$X_f = \tfrac{1}{2}(T_{f-}-T_{f+}) < 0, \tag{14}$$

an impossibility. To ensure that T_{f+} is close to the flame temperature, and hence that the temperature gradient is small on the hotter side, set

$$2Y_f = T_{f+}-T_{f-} + k/\theta \text{ with } k = \text{const.} \tag{15}$$

In seeking an asymptotic solution as $\theta \to \infty$ we shall assume that equilibrium prevails for $x > x_*$ even though T does not rise above T_* by an $0(1)$ amount there, and check a posteriori that the solution thereby constructed is self-consistent.

In view of the assumption (15), the Shvab-Zeldovich relations (5b) becomes

$$T + 2Y = T_{f+} +(k/2\theta)\operatorname{erfc}(x) \tag{16}$$

and, hence,

$$T = T_{f+} + (k/2\theta)\operatorname{erfc}(x) \quad \text{for} \quad x > x_*, \tag{17}$$

since $Y = 0$ there. To complete the description of the combustion field outside the reaction zone, we need the temperature in the frozen region ahead of the flame sheet, i.e. the linear combination of 1 and $\operatorname{erf}(x)$ that takes on the values T_{f-} at $x = -\infty$ and T_* at $x = x_*$; clearly

$$T = \{T_{f-}[\mathrm{erfc}(-x_*)-\mathrm{erfc}(-x)] + T_*\mathrm{erfc}(-x)\}/\mathrm{erfc}(-x_*) \text{ for } x < x_* . \quad (18)$$

This, like the result (17), is correct to any order in θ^{-1}, provided T_* is determined to the same order. We shall only need leading-order accuracy in the result (18), so that taking

$$T_* = T_{f+} \quad (19)$$

is good enough. Determination of the non-expandable x_* comes from analysis of the reaction zone, for which the leading-order result

$$X_* = \tfrac{1}{2}(T_{f-}-T_{f+})\mathrm{erfc}(x_*)+\tfrac{1}{2}X_f\mathrm{erfc}(-x_*), \quad (20)$$

a consequence of the Shvab-Zeldovich relation (5a), is needed.

The appropriate variable in the reaction zone is

$$\xi = \theta(x-x_*), \quad (21)$$

so that coefficients in the layer expansion

$$T = T_{f+} - \theta^{-1}T_{f+}^2\phi +\ldots \qquad \text{with} \quad \phi = (1/T)_1 \quad (22)$$

are considered to be functions of ξ. The Shvab-Zeldovich relation (5b) gives

$$Y = \tfrac{1}{2}\theta^{-1}T_{f+}^2(\phi-\phi_*)+\ldots \text{ with } \phi_* = -k\ \mathrm{erfc}(x_*)/2T_{f+}^2, \quad (23)$$

so that the structure equation is

$$d^2\phi/d\xi^2 = \tilde{\mathcal{D}}(\phi-\phi_*)e^{-\phi} \text{ with } \tilde{\mathcal{D}} = \mathcal{D}X_*e^{-\theta/T_{f+}}/2\theta^2. \quad (24)$$

Note that $\tilde{\mathcal{D}} = O(1)$ implies $\mathcal{D}e^{-\theta/T} = O(\theta^2)$ for $x > x_*$: there must be the equilibrium $Y = 0$ on the right of the flame sheet since otherwise

the reaction term in the Y-equation could not be balanced there. In other words, our solution is self-consistent.

Equation (24) is precisely the structure equation for the premixed flames discussed in section 2.4. Since the gradient dT/dx vanishes on the right of the flame sheet, it determines the gradient on the left (as was explained in section 2.5). But the latter is known in terms of x_* from the expression (18), so the result is an equation for x_*, namely

$$\frac{2(T_{f+}-T_{f-})}{\sqrt{\pi}} \cdot \frac{e^{-x_*^2}}{\operatorname{erfc}(-x_*)} = \frac{T_{f+}^2\sqrt{DX_*}e^{-\phi_*/2}}{\theta e^{\theta/2T_{f+}}} . \qquad (25)$$

When the definition (20) is used to eliminate X_*, equations (23) and (25) give ϕ_* (representing, when it is negative, the maximum temperature in the combustion field) and D as functions of x_*, i.e. the required relation between the maximum temperature and the Damköhler number.

The corresponding response curve is shown in figure 3 for several positive values of the constant k; when k is non-positive, the maximum temperature is T_{f+} and not $T_{f+}-\theta^{-1}T_{f+}^2\phi_*$. For k sufficiently small, the response is monotonic; otherwise it is S-shaped. Responses in the shape of an S appear to be associated with a flux of heat away from the flame sheet on both sides, but this has never been proved.

3. General Extinction Analysis.

We turn now to the question of extinction in general, i.e. when there is an O(1) heat flux away from the flame sheet in both directions. It is found that the flame temperature on the whole upper branch of the S-response differs by $O(\theta^{-1})$ from the Burke-Schumann value (12) at its end; our

extinction analysis will use this fact. Because of the O(1) drop in temperature away from the flame sheet, the combustion field on each side is now frozen; nevertheless, the leading-order solution outside the reaction zone is identical to the equilibrium solution constructed in the limit $\mathcal{D} \to \infty$ (section 1). Thus, the results (10), which follow from equilibrium and the Shvab-Zeldovich relations, hold for T_0, X_0, Y_0. Finally, before considering the flame-sheet structure, we define x_* and T_* by the formulas (11) and (12).

In the reaction zone, the variable (21) and expansion (22) still apply, while the Shvab-Zeldovich relations gives

$$X = \tfrac{1}{2}\theta^{-1}T_*^2(\phi+A\xi)+\ldots, \quad Y = \tfrac{1}{2}\theta^{-1}T_*^2(\phi+B\xi)+\ldots, \tag{26}$$

where

$$A = (T_{f+}-T_{f-}+2X_f)e^{-x_*^2}/\sqrt{\pi}T_*^2 > 0, \quad B = (T_{f+}-T_{f-}-2Y_f)e^{-x_*^2}/\sqrt{\pi}T_*^2 < 0; \tag{27}$$

the signs of A and B follow from the requirement that the flame temperature be larger than the temperatures at both $-\infty$ and $+\infty$. The temperature equation therefore reduces to

$$d^2\phi/d\xi^2 = \tilde{\mathcal{D}}(\phi+A\xi)(\phi+B\xi)e^{-\phi} \text{ with } \tilde{\mathcal{D}} = T_*^2\mathcal{D}e^{-\theta/T_*}/4\theta^3, \tag{28}$$

under the boundary conditions

$$d\phi/d\xi = -A+\ldots \text{ as } \xi \to -\infty, \quad d\phi/d\xi = -B+\ldots \text{ as } \xi \to +\infty, \tag{29}$$

which come from matching the leading terms in the expansions (26) with

$$X_0 = 0 \text{ for } x < x_* \text{ and } Y_0 = 0 \text{ for } x > x_* . \tag{30}$$

The problem (28), (29) determines the minimum value ϕ_m (i.e. the maxiumum temperature in the combustion field) as a function of $\tilde{\mathcal{D}}$. It can be reduced to canonical form by writing

$$\tilde{\phi} = \phi + \tilde{\gamma}\tilde{\xi}, \quad \tilde{\xi} = (A-B)\xi/2 \quad \text{with} \quad \tilde{\gamma} = (A+B)/(A-B); \tag{31}$$

we find

$$d^2\tilde{\phi}/d\tilde{\xi}^2 = \tilde{\mathcal{D}}_e(\tilde{\phi}^2 - \tilde{\xi}^2)e^{-\tilde{\phi}+\tilde{\gamma}\tilde{\xi}} \quad \text{with} \quad \tilde{\mathcal{D}}_e = 4\tilde{\mathcal{D}}/(A-B)^2 \tag{32}$$

and

$$d\tilde{\phi}/d\tilde{\xi} = -1+\ldots \text{ as } \tilde{\xi} \to -\infty, \quad d\tilde{\phi}/d\tilde{\xi} = 1+\ldots \text{ as } \tilde{\xi} \to +\infty. \tag{33}$$

Various responses determined by numerical integration of the problem (32), (33) are shown in figure 4; these C-shaped curves correspond to the neighborhood of the point E in figure 2. Note that $A > 0$, $B < 0$ imply

$$-1 < \tilde{\gamma} < 1. \tag{34}$$

Certain limiting forms of this problem as $\tilde{\mathcal{D}}_e \to \infty$ are of interest.

(i) The Burke-Schumann limit

$$d^2\hat{\phi}/d\hat{\xi}^2 = (\hat{\phi}^2 - \hat{\xi}^2), \quad d\hat{\phi}/d\hat{\xi} = \mp 1+\ldots \text{ as } \hat{\xi} \to \mp\infty \tag{35}$$

is obtained by setting

$$\tilde{\phi} = \tilde{\mathcal{D}}_e^{-1/3}\hat{\phi}, \quad \tilde{\xi} = \tilde{\mathcal{D}}_e^{-1/3}\hat{\xi}. \tag{36}$$

This is the structure problem for the equilibrium solution discussed at the end of section 1; it applies far to the right on the upper branch in figure 4. Existence and uniqueness have recently been proved by Holmes.

(ii) The so-called premixed-flame limit results on defining a small parameter ε by

$$\varepsilon^{1\mp\tilde{\gamma}}\ln(1/\varepsilon) = D_e^{-1} \quad \text{according as} \quad \tilde{\gamma} \gtrless 0 \tag{37}$$

and putting

$$\tilde{\phi} = \hat{\phi} - \ln\varepsilon, \quad \tilde{\xi} = \hat{\xi} \mp \ln\varepsilon. \tag{38}$$

We find

$$d^2\hat{\phi}/d\hat{\xi}^2 = 2(\hat{\phi}+\tilde{\xi})e^{-\hat{\phi}+\tilde{\gamma}\hat{\xi}} \tag{39}$$

and the boundary conditions (35b); existence of the solution requires changing from one equation to the other when the sign of $\tilde{\gamma}$ is changed. The relevance of this structure problem to the lower branch in figure 4 is discussed below.

(iii) The so-called partial-burning limit corresponds to

$$\tilde{\gamma} = 0. \tag{40}$$

Defining ε by

$$\varepsilon^{-2}e^{-1/\varepsilon} = D_e^{-1} \tag{41}$$

and setting

$$\tilde{\phi} = \hat{\phi} + 1/\varepsilon, \quad \tilde{\xi} = \hat{\xi} \tag{42}$$

gives

$$d^2\hat{\phi}/d\hat{\xi}^2 = e^{-\hat{\phi}} \tag{43}$$

and the boundary conditions (35a). Cases (ii) and (iii) apply on the lower branch in figure 4 and correspond to the X-perturbation becoming large ($\tilde{\gamma} > 0$), the Y-perturbation becoming large ($\tilde{\gamma} < 0$), and the two perturbations becoming large simultaneously

($\tilde{\gamma} = 0$). They are of interest because every point on the middle branch of the S in figure 2 that is not too close to E or I corresponds to a solution for which the flame-sheet structure has one of these three forms. As an example we shall now demonstrate the general applicability of case (iii).

4. Partial-Burning Branch

This part of the S is characterized by O(1) values of X_* and Y_*, hence the term partial-burning. It is convenient to prescribe the flame temperature T_* (also the maximum temperature) and calculate $\mathcal{D}$, rather than vice-versa.

On either side of the flame sheet the leading-order temperature is

$$T_0 = T_{f\mp} + (T_* - T_{f\mp})\operatorname{erfc}(\mp x)/\operatorname{erfc}(\mp x_*) \text{ for } x \lesssim x_*. \tag{44}$$

In order to determine x_*, we anticipate a conclusion to be drawn from the flame-sheet structure, to wit

$$\frac{dT}{dx}(x_*-0) + \frac{dT}{dx}(x_*+0) = 0; \tag{45}$$

this gives

$$\operatorname{erfc}(x_*)/\operatorname{erfc}(-x_*) = (T_* - T_{f+})(T_* - T_{f-}). \tag{46}$$

The Shvab-Zeldovich relations (5) then determine X_* and Y_*.

In the reaction zone, the variable (21) and expansion (22) still apply, so that the structure equation is

$$d^2\phi/d\xi^2 = \tilde{\mathcal{D}}e^{-\phi} \text{ with } \tilde{\mathcal{D}} = \mathcal{D}X_*Y_*e^{-\theta/T_*}/T_*^2\theta, \tag{47}$$

which is equivalent to the equation (43). A single integration shows that the derivative $d\phi/dx$ takes equal but opposite values at $\xi = \pm\infty$, the origin

of the relation (45). No information is obtained about $\mathcal{D}$, however, except that it is proportional to e^{θ/T_*} and therefore a rapidly decreasing function of T_*; to determine it requires an examination of higher-order terms.

This structure is appropriate for the lower part of the middle branch. As T_* increases on moving up the branch, one of the mass fractions X_* or Y_* decreases to zero; therefore, a different structure takes over, characterized by $O(\theta^{-1})$ values of one of the mass fractions but still $O(1)$ values of the other. One or other of the equations (39) then governs; again $\mathcal{D}$ is proportional to e^{θ/T_*}. Further increase in T_* towards the Burke-Schumann value (12) causes the remaining $O(1)$ mass fraction to decrease until the structure (32), (33) is attained. We forego further discussion of the middle branch since it corresponds to unstable solutions, our final topic.

5. Stability.

The middle branch has long been believed to be unstable, but only recently has the matter been confirmed mathematically. To do so, the problem must be examined on a time scale that is relevant to the reaction zone, i.e. using a fast time

$$\tau = \theta^2 t. \tag{48}$$

The governing equations (2) show that

$$\partial T/\partial\tau = \partial X/\partial\tau = \partial Y/\partial\tau = 0 \tag{49}$$

everywhere on the two sides of the flame sheet: T, X, and Y are described to all orders by the steady state.

On the other hand, in the reaction zone the time derivatives are as important as the diffusion terms, so that equation (28) becomes

$$\partial^2\tilde{\phi}/\partial\xi^2 - \partial\phi/\partial\tau = \tilde{\mathcal{D}}(\phi+A\xi)(\phi+B\xi)e^{-\phi}. \qquad (50)$$

Correspondingly, equation (32) is replaced by

$$\partial^2\tilde{\phi}/\partial\tilde{\xi}^2 - \partial\tilde{\phi}/\partial\tilde{\tau} = \tilde{\mathcal{D}}_e(\tilde{\phi}^2-\tilde{\xi}^2)e^{-\tilde{\phi}+\tilde{\gamma}\tilde{\xi}} \quad \text{with } \tilde{\tau} = (A-B)^2\tau/4. \qquad (51)$$

Infinitesimal disturbances $e^{\lambda\tilde{\tau}}\tilde{\phi}_1$ of the steady state $\tilde{\phi}_0$, which is the solution of the problem (32), are then described by the eigenvalue problem

$$\tilde{\phi}_1'' + [V(\tilde{\xi})-\lambda]\tilde{\phi}_1 = 0, \quad \tilde{\phi}_1 \to 0 \text{ as } \tilde{\xi} \to \pm\infty, \qquad (52)$$

where

$$V = \tilde{\mathcal{D}}_e(\tilde{\phi}_0^2-2\tilde{\phi}_0-\tilde{\xi}^2)e^{-\tilde{\phi}_0+\tilde{\gamma}\tilde{\xi}}. \qquad (53)$$

(Attention is restricted to disturbances satisfying the Shvab-Zeldovich relations.)

This problem has been treated by Taliaferro, Buckmaster & Nachman (1983) who show, in particular, that the transition from stable solutions on the upper branch to unstable solutions on the middle branch occurs exactly at the static extinction point E in figure 2. (The rigorous part of the analysis is due to Taliaferro.) Stability on the upper branch is typified by the Burke-Schumann limit (35), for which the corresponding eigenvalue problem is

$$\hat{\phi}_1'' - (2\hat{\phi}_0+\hat{\lambda})\hat{\phi}_1 = 0 \quad \text{with } \hat{\lambda} = \mathcal{D}_e^{-2/3}\lambda, \quad \hat{\phi}_1 \to 0 \text{ as } \hat{\xi} \to \pm\infty. \qquad (54)$$

Instability on the middle branch is exemplified by the premixed-flame and partial-burning limits (39) and (43). For the former the eigenvalue problem is

$$\hat{\phi}_1'' - [2(1\pm\hat{\xi}-\hat{\phi}_0)e^{-\hat{\phi}_0+\tilde{\gamma}\hat{\xi}}+\lambda]\hat{\phi}_1 = 0 \qquad (55)$$

under the boundary conditions (54b); for the latter it is

$$\hat{\phi}_1'' + (e^{-\hat{\phi}_0}-\lambda)\hat{\phi}_1 = 0 \qquad (56)$$

under the same boundary conditions.

Standard treatments show that the spectrum of λ is negative if $\hat{\phi}_0$ is everywhere positive, and that is ensured by the property $\hat{\phi}_0 > |\hat{\xi}|$ of the steady state. Peters was the first to show, albeit numerically, that the problems (55) have eigenvalues with positive real part. (Peters writes equations in a slightly different way from ours; his m is equivalent to $2(1-|\tilde{\gamma}|)$ and so is positive.) Matalon and Ludford noted, in a different context, that the problem (56) has a positive eigenvalue. Indeed, the steady state is

$$\hat{\phi}_0 = \ell n[2\cosh^2\tfrac{1}{2}(\hat{\xi}-\hat{\xi}_m)], \qquad (57)$$

where $\hat{\xi}_m$ is an integration constant giving the location of the maximum temperature, so that

$$\lambda = \tfrac{1}{4},\ \hat{\phi}_1 = \operatorname{sech}\tfrac{1}{2}(\hat{\xi}-\hat{\xi}_m) \qquad (58)$$

are seen to be an eigenvalue and its corresponding eigenfunction.

6. The Ignition Point.

The neighborhood of the point I in figure 2 can be analyzed by considering perturbations of the frozen solution that raise the maximum temperature by an $O(\theta^{-1})$ amount. A similar analysis in the context of spherical diffusion flames will be given in the next lecture, so we omit the discussion for counterflow flames. The stability of the lower branch

has not yet been examined, but the conclusions must agree with the instability result for the partial-burning portion of the middle branch.

References

1. Taliaferro, S., Buckmaster, J., & Nachman, A. (1983). The fast-time instability of diffusion flames. (Submitted for publication.)

Captions

8.1 Notation for the counterflow diffusion flame.

8.2 Ignition and extinction for S-shaped response.

8.3 Steady-state responses when the temperature gradient in positive for $x > 0$ and small for $x < 0$, the latter being representative by K. Drawn for $X_f = \frac{1}{2}(T_{f+} - T_{f-})$.

8.4 Extinction curves. For $|\tilde{\gamma}| \geq 1$ no turning point is found numerically, a result that still lacks formal proof.

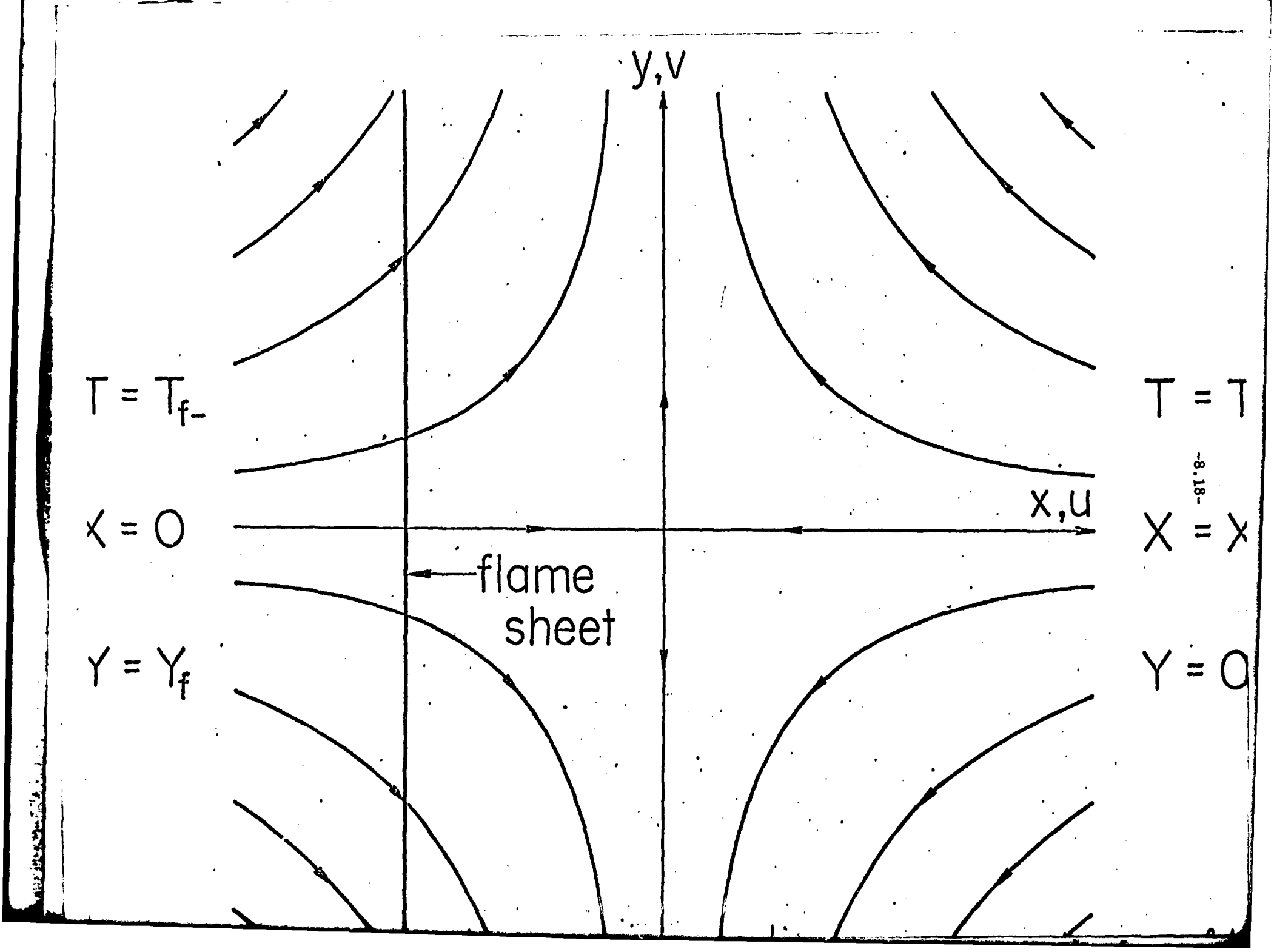
y,v
T = T_f-
T = T
x,u
X = 0
X = X
flame
sheet
Y = Y_f
Y = 0

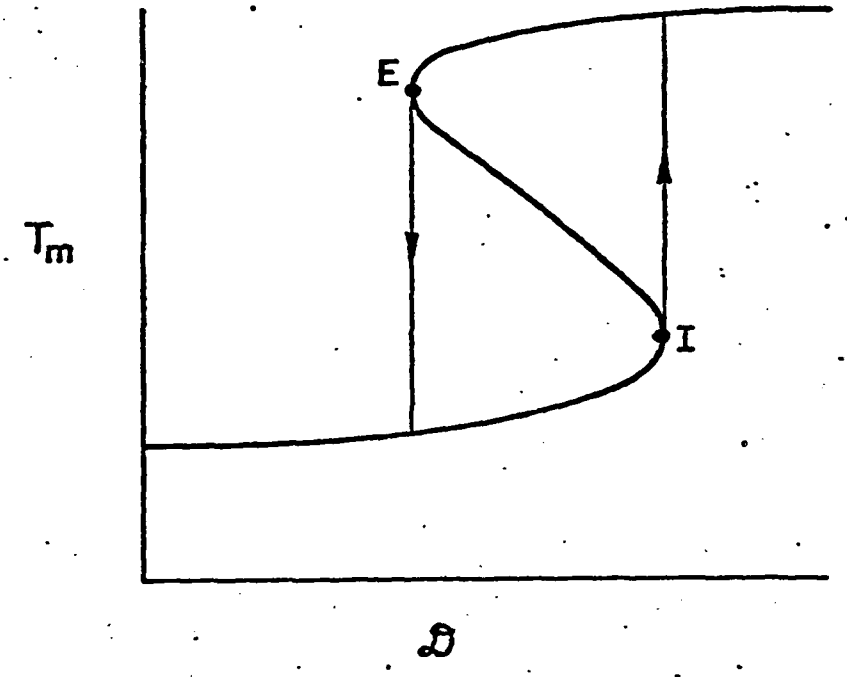
E
I
T_m
$\mathcal{D}$

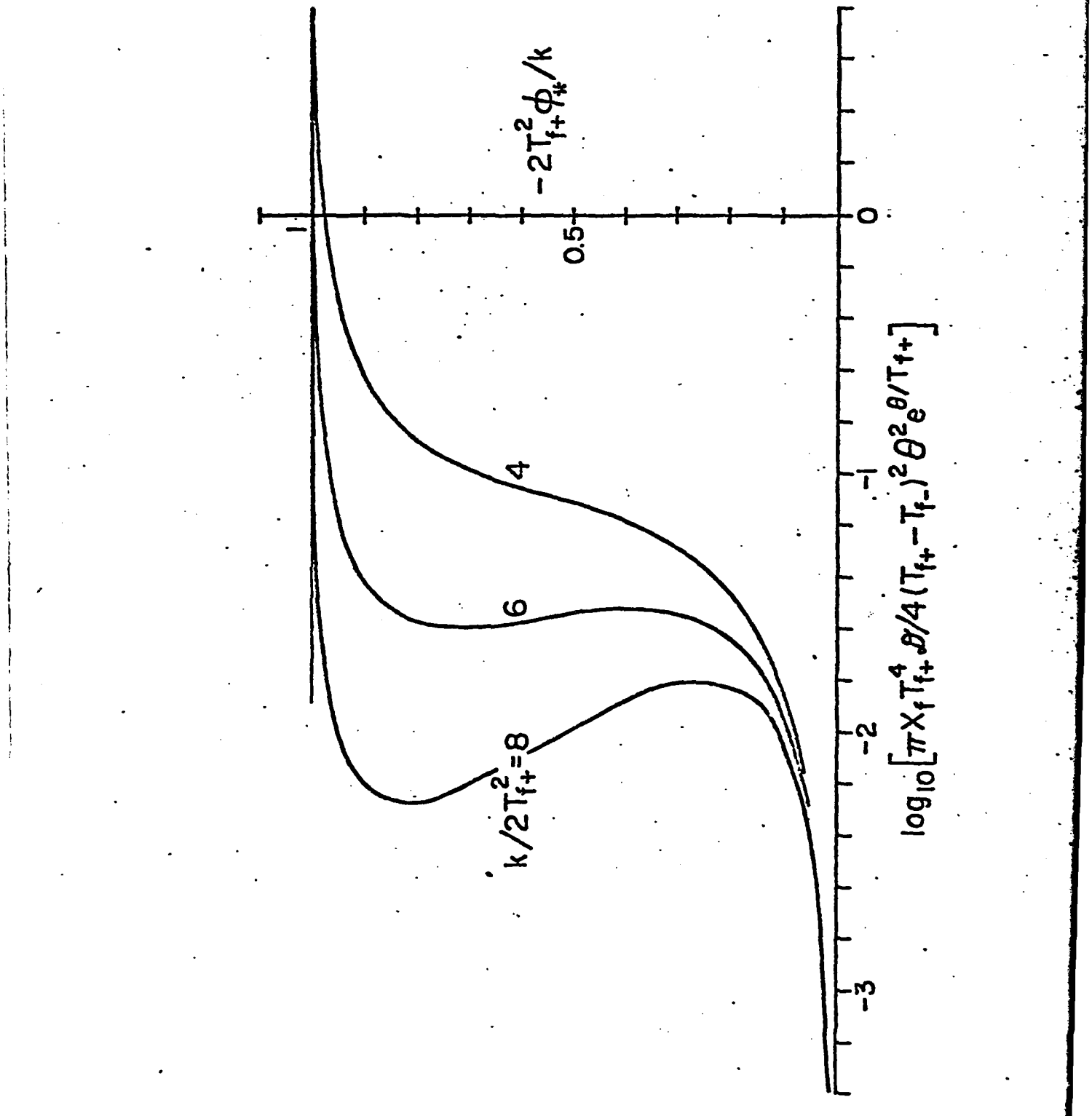
$-2T_{f+}^2\phi_*/k$
1
0.5
0
-1
-2
-3
$\log_{10}[\pi X_f T_{f+}^4 \mathcal{B}/4(T_{f+}-T_{f-})^2\theta^2 e^{\theta/T_{f+}}]$
4
6
$k/2T_{f+}^2=8$

4.3

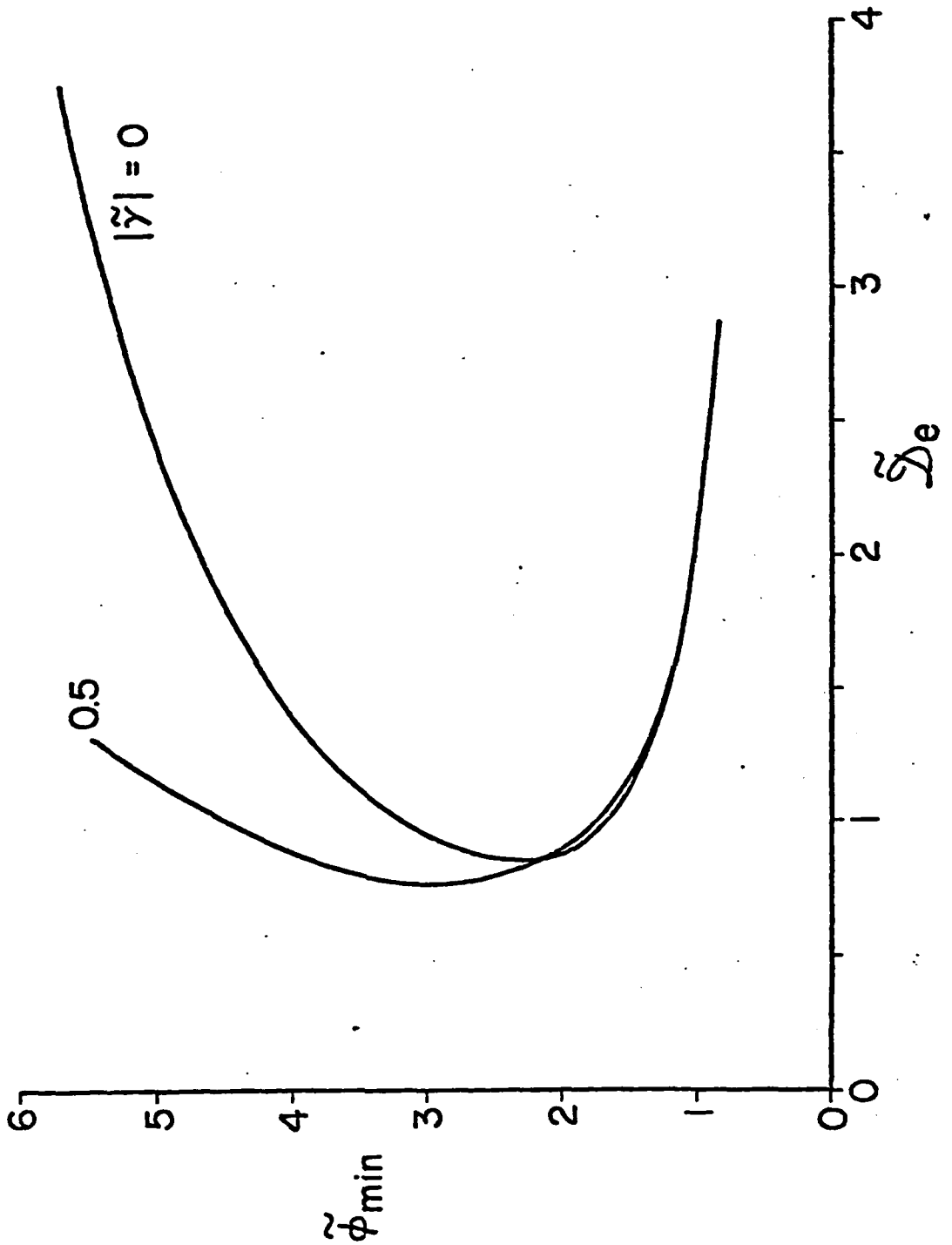

8.4

SECURITY CLASSIFICATION OF THIS PAGE (When Data Entered)

REPORT DOCUMENTATION PAGE		READ INSTRUCTIONS BEFORE COMPLETING FORM
1. REPORT NUMBER 153	2. GOVT ACCESSION NO. AD-A129 914	3. RECIPIENT'S CATALOG NUMBER
4. TITLE (and Subtitle) LECTURES ON MATHEMATICAL COMBUSTION Lecture 8: Counterflow Diffusion Flames		5. TYPE OF REPORT & PERIOD COVERED Interim Technical Report 6. PERFORMING ORG. REPORT NUMBER
7. AUTHOR(s) J.D. Buckmaster & G.S.S. Ludford		8. CONTRACT OR GRANT NUMBER(s) DAAG29-81-K-0127
9. PERFORMING ORGANIZATION NAME AND ADDRESS Department of Theoretical and Applied Mechanics Cornell University, NY 14853		10. PROGRAM ELEMENT, PROJECT, TASK AREA & WORK UNIT NUMBERS P-18243-M
11. CONTROLLING OFFICE NAME AND ADDRESS U. S. Army Research Office Post Office Box 12211 Research Triangle Park, NC 27709		12. REPORT DATE January 1983 13. NUMBER OF PAGES 21
14. MONITORING AGENCY NAME & ADDRESS(if different from Controlling Office)		15. SECURITY CLASS. (of this report) Unclassified 15a. DECLASSIFICATION/DOWNGRADING SCHEDULE

16. DISTRIBUTION STATEMENT (of this Report)

Approved for public release: distribution unlimited.

17. DISTRIBUTION STATEMENT (of the abstract entered in Block 20, if different from Report)

18. SUPPLEMENTARY NOTES

THE VIEW, OPINIONS, AND/OR FINDINGS CONTAINED IN THIS REPORT ARE THOSE OF THE AUTHOR(S) AND SHOULD NOT BE CONSTRUED AS AN OFFICIAL DEPARTMENT OF THE ARMY POSITION, POLICY, OR DECISION, UNLESS SO DESIGNATED BY OTHER DOCUMENTATION.

19. KEY WORDS (Continue on reverse side if necessary and identify by block number)

NA

20. ABSTRACT (Continue on reverse side if necessary and identify by block number)

The fundamental characteristic of diffusion flames is that the two reactants, fuel and oxidizer, are supplied in different parts of the combustion field, so that they must come together and mix by diffusion before reaction can take place. Counterflowing streams provide one method of bringing them together; the resulting diffusion flames, whose main properties were established by Linan, is the subject of this lecture.

DD FORM 1 JAN 73 1473 EDITION OF 1 NOV 65 IS OBSOLETE

SECURITY CLASSIFICATION OF THIS PAGE (When Data Entered)


DA
FIL